



OPEN ACCESS

EDITED BY

Ki-Yong Oh,
Hanyang University, Republic of Korea

REVIEWED BY

Chuanyu Sun,
University of Padua, Italy
Srinivasarao Gorantla,
Technology and Research, India

*CORRESPONDENCE

Jaeyoung Kim,
✉ korean4u@korea.ac.kr

RECEIVED 14 October 2025

REVISED 14 November 2025

ACCEPTED 29 November 2025

PUBLISHED 05 January 2026

CITATION

Song H and Kim J (2026) Method for applying OCV tables to enhance SOC accuracy after small discharges.

Front. Energy Res. 13:1724766.

doi: 10.3389/fenrg.2025.1724766

COPYRIGHT

© 2026 Song and Kim. This is an open-access article distributed under the terms of the [Creative Commons Attribution License \(CC BY\)](https://creativecommons.org/licenses/by/4.0/). The use, distribution or reproduction in other forums is permitted, provided the original author(s) and the copyright owner(s) are credited and that the original publication in this journal is cited, in accordance with accepted academic practice. No use, distribution or reproduction is permitted which does not comply with these terms.

Method for applying OCV tables to enhance SOC accuracy after small discharges

Hyunchul Song ^{1,2} and Jaeyoung Kim^{1*}

¹Program in Converging Technology System Standardization, Korea University, Seoul, Republic of Korea, ²Department of Green Energy Engineering, Far East University, Chungbuk, Republic of Korea

Lithium-ion batteries are widely used as core energy sources in various applications such as electric ships, drones, electric vehicles (EVs), and energy storage systems (ESSs). These batteries can be operated safely with the help of a Battery Management System (BMS). Among the various functions of the BMS, accurately estimating the State of Charge (SOC) is crucial for the efficient use of the battery. One common method for improving SOC estimation accuracy involves using an Open Circuit Voltage (OCV) table. The OCV table is typically divided into a charge OCV table and a discharge OCV table, both of which can be used to correct SOC values. Generally, the charge OCV table is applied after charging, while the discharge OCV table is used after discharging. However, when a small amount of discharge occurs after charging, SOC correction using a simple OCV table may not yield accurate results. In this paper, we examine SOC estimation using both the charge and discharge OCV tables in cases of minor discharge following a charging cycle. We also implemented and tested an optimal compensation logic designed to improve SOC accuracy by evaluating the error associated with each method. The test results show that the proposed logic reduced the SOC estimation error to 1.4% when a 3% discharge occurred without a rest period, and to 1.6% when the same discharge occurred after a 2-h rest. This logic enables accurate SOC estimation even under conditions involving small discharges after charging, thereby enhancing overall estimation reliability.

KEYWORDS

lithium-ion battery, battery-management-system, state-of-charge, open circuit voltage table, small discharge, charge/discharge hysteresis, error reduction, thevenin equivalent circuit

1 Introduction

While lithium-ion batteries do not directly reduce carbon emissions, they play a crucial role in supporting the electrification of the transportation sector and enabling the efficient and stable utilization of intermittent renewable energy sources such as solar and wind power (Chatzigeorgiou and Papadopoulos, 2024). Therefore, lithium-ion batteries are regarded as a key component of the infrastructure required to achieve carbon neutrality. These batteries are widely used in various fields such as aviation, drones, electric ships (Ku et al., 2015; Misyris et al., 2017), and electric vehicles (EVs), and their applications continue to expand. In EVs, lithium-ion batteries serve as the primary power source, and extensive research and development are being conducted to extend the driving range. Efficient use of lithium-ion batteries can lead to increased

driving range, making accurate estimation of the battery's State of Charge (SOC) a critical factor.

The Battery Management System (BMS) is a system that comprehensively manages lithium-ion batteries. In automotive applications, it is often divided into the Battery Management Unit (BMU) and the Cell Management Unit (CMU). The CMU monitors cell voltage, temperature, and current and transmits this data to the BMU, which in turn uses this information to estimate the battery's State of Charge (SOC) and State of Health (SOH) (Lu et al., 2013). Additionally, the BMS performs fault diagnosis and controls the main power relay to interrupt charging or discharging as necessary (Gabbar et al., 2021). It also performs cell balancing when voltage deviation occurs between cells (Omariba et al., 2019).

The driving range of an electric vehicle is closely related to the accuracy of SOC estimation. One widely used method for estimating SOC is the coulomb counting method (Ng et al., 2009), and to correct accumulated errors, an Open Circuit Voltage (OCV)-based correction method is often employed (Zhang et al., 2016; LEE et al., 2007). Other methods include equivalent circuit modeling (Lee et al., 2005) and internal resistance-based models (Sato and Kawamura, 2002), such as recursive estimation using Kalman filters (Shrivastava et al., 2019; Zhang et al., 2019). Among these, the OCV-based correction method is the most fundamental (Jeong et al., 2013). OCV-SOC tables can be provided by battery manufacturers or obtained by performing controlled charge-discharge cycles.

The discharge OCV table is generally constructed by discharging the battery in increments of 5% or 10% from a fully charged state under standard conditions, with measurements taken after the cell voltage has stabilized. Although a minimum rest time of 30 min is required for stabilization (Yang et al., 2017), a rest period of 2 h is commonly used for optimal stability (Zhou et al., 2020; Xiong et al., 2011). Conversely, the charge OCV table is constructed by charging in increments from a fully discharged state, with measurements also taken after a rest period of at least 2 h. These OCV tables remain valid even as the battery degrades over time, making them reusable.

In practice, the OCV table can be used to correct SOC by measuring stabilized cell voltage during rest periods. In Energy Storage Systems (ESS), such rest periods are common during discharge and make frequent corrections feasible. In EVs, OCV-based correction is possible during extended idle periods or while parked. Previous studies have focused on SOC correction using OCV in short rest periods during battery operation (Jeong et al., 2014; Zhou et al., 2023), where full stabilization is difficult. In contrast, this study focuses on SOC correction during non-operating periods of lithium-ion batteries, such as nighttime idle periods in ESS or after slow charging in EVs.

In residential settings such as apartment complexes, EVs are often charged using slow chargers while parked. In many cases, the charging plug remains connected for extended periods. In electric vehicles, the battery thermal management system operates not only during slow charging but also during fast charging, maintaining the cell temperature within a safe range (Dai et al., 2023). To enhance safety and prevent fires, the BMS may periodically activate during parking to check battery status. In such scenarios, it is possible to use the stabilized cell voltage after charging to correct SOC via the OCV table.

Similarly, in ESS applications, nighttime rest periods can include small discharges due to minimal system use. In addition, due to the recent large-scale installation of electric vehicle charging stations, many apartments and multi-family housing complexes now have charging stations within their premises. Even in places where they are not available, there are often charging locations within a 10-min drive, allowing residents to move their cars back home after charging. After such events, if the SOC is inaccurate, an accurate SOC correction based on the OCV is required. However, it is unclear whether the charge OCV table (used before the discharge) or the discharge OCV table (following the small discharge) should be applied. This choice affects the SOC correction results, and a rational decision is essential.

This study investigates whether SOC correction should use the charge or discharge OCV table after small discharges that follow charging. Tests were conducted under two conditions: one with a 2-h rest period before a 3% discharge (Song, 2025), and another with immediate discharge after charging. Based on these tests and prior research (Song, 2025), additional experiments were performed to generate new findings. Furthermore, SOC correction logic using both charge and discharge OCV tables was implemented and evaluated. This study aims to propose an improved method for applying OCV tables to enhance SOC estimation accuracy in lithium-ion battery systems.

2 Main body

2.1 Coulomb counting method

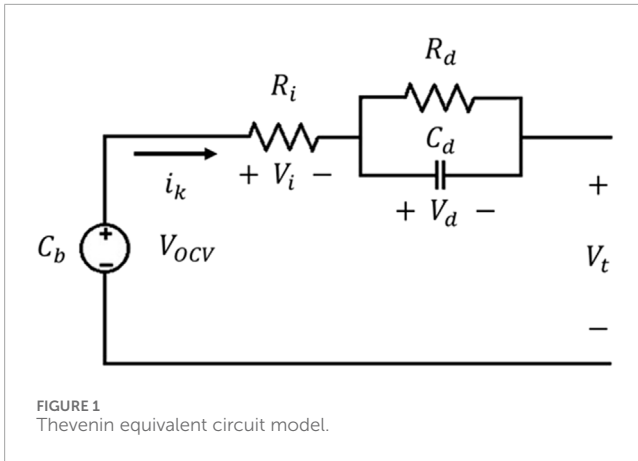
The most used method for estimating the State of Charge (SOC) is the Coulomb counting method. This method can be expressed as shown in Equation 1. In addition to SOC estimation, the Coulomb counting method is also widely used for calculating the State of Health (SOH) of batteries (Song et al., 2025).

$$SOC(t) = SOC(t_0) - \frac{1}{C_b} \int_{t_0}^t i(\tau) d\tau \quad (1)$$

In Equation 1, $SOC(t_0)$ represents the initial state of charge (SOC), and C_b denotes the Full Charge Capacity. The SOC is calculated by subtracting the accumulated current, divided by the C_b , from the initial SOC value. However, if there is a measurement error in the current integration, the error may accumulate over time, leading to an increasing deviation in the final SOC value. To correct this, a widely used method involves utilizing the OCV (Open Circuit Voltage) table during a resting period when the battery is neither charging nor discharging. This method allows for accurate SOC correction by referencing the stable voltage characteristics of the battery.

2.2 SOC estimation with Extended Kalman Filter (EKF)

Figure 1 illustrates the Thevenin equivalent circuit model used for SOC estimation based on the Extended Kalman Filter (EKF) (Cui et al., 2022). Equations 2, 3 represent the discrete-time state-space model derived from the Thevenin equivalent model for



SOC estimation using EKF. By applying this model to the EKF, the SOC can be estimated. Equation 3 corresponds to the output equation of the Thevenin equivalent circuit in the EKF method, where $OCV(SOC_k)$ is calculated by extracting the OCV value corresponding to the predicted SOC using the OCV table. This allows for the prediction of the terminal voltage V_t , which is then compared with the actual measured terminal voltage to estimate the system state. As such, the OCV table is an essential component in EKF-based SOC estimation. The choice between using a charging or discharging OCV table can affect the estimation accuracy.

In this study, Thevenin model parameters such as R_i , R_d , and C_d were selected based on manufacturer specifications and fine-tuned using experimental data under nominal conditions. However, these parameters may vary with SOC, SOH, and temperature. To improve the accuracy and generality of the EKF, future work will include a more rigorous parameter identification process, such as the Hybrid Pulse Power Characterization (HPPC) test protocol, to extract these values under varying conditions.

$$\begin{bmatrix} SOC_k \\ V_{d,k} \end{bmatrix} = \begin{bmatrix} 1 & 0 \\ 0 & e^{-\frac{\Delta t}{R_d C_d}} \end{bmatrix} \times \begin{bmatrix} SOC_{k-1} \\ V_{d,k-1} \end{bmatrix} + \begin{bmatrix} -\frac{\Delta t}{C_b} \\ R_d \left(1 - e^{-\frac{\Delta t}{R_d C_d}} \right) \end{bmatrix} i_{k-1} \quad (2)$$

$$V_t = V_{ocv}(SOC_k) - i_k R_i - V_{d,k} \quad (3)$$

2.3 Charge and discharge OCV table

In this study, tests were conducted using the Samsung SDI 21700 battery cell, which is based on Nickel Cobalt Aluminum Oxide (NCA) chemistry. Unlike LFP cells, NCA-based cells exhibit a steeper and more nonlinear OCV-SOC curve, which enables more accurate voltage-based SOC estimation. The OCV (Open Circuit Voltage) tables utilized were based on the specifications provided by the battery manufacturer. To construct the tables, standard charge and discharge procedures were followed: the battery was fully charged and fully discharged and then charged or discharged in 5% SOC (State of Charge) increments. At each step, the stabilized cell voltage was measured and recorded as the OCV. These

measurements were conducted at room temperature (25 °C), and the resulting data were organized into separate charge and discharge OCV tables.

The OCV tables serve as critical reference data for estimating SOC in battery management systems (BMS). Since the manufacturer does not provide specific calibration methods for these tables, users are responsible for applying appropriate corrections based on their system and environmental conditions. Typically, the charge OCV table is used during charging processes, while the discharge OCV table is used during discharging. However, since it is more important for the user to match the accuracy of the SOC during discharge rather than during charging, sometimes only one discharge OCV table is used.

Figure 2 is a charge and discharge OCV Table graph measured at room temperature (25 °C). In Figure 2, the charge OCV and discharge OCV show slight differences across the entire range, and the difference is particularly large below SOC 40%. Among them, the deviation between the charge and discharge OCV in the SOC 5% part is a maximum difference of 153 mV. Since this voltage difference between the charge OCV and discharge OCV appears directly as a deviation in the SOC, it can affect the SOC accuracy.

Although the OCV hysteresis observed in this study is treated empirically through separate charge and discharge tables, it is known to originate from mechanisms such as phase transitions in the anode material and lithium-ion diffusion gradients (Ovejas et al., 2019; Barai et al., 2015). A detailed electrochemical analysis will be considered in future work to further clarify these effects.

While this study adopts a practical approach based on the Thevenin equivalent circuit and empirical OCV tables, future work may consider integrating electrochemical modeling techniques such as simplified P2D models or multi-scale frameworks to further investigate the microscopic origins of OCV hysteresis and improve the physical interpretability of the SOC-OCV mapping.

2.4 Small discharge test after charging

The electric vehicle slow charger is generally 3–7 kW, and the full charging time may vary depending on the pack capacity, but it takes approximately 4–5 h. Based on this, the current flowing per cell may vary depending on the series and parallel configuration of the cells in the pack, but the charging was performed at 0.2 C to simulate a 4-to-5-h slow charge. The small discharge was set to 3% of the capacity based on a short discharge of less than 10 min. First, to confirm the standard capacity, the standard charge (0.5 C) and standard discharge (0.2 C) were performed based on the specification, and the discharge capacity was confirmed to be 4808.6506mAh. Therefore, the impact of a small discharge of 3% based on the standard discharge capacity was confirmed.

For the small-discharge test after charging, tests without a rest period and tests with a rest period between the charge and the small-discharge were performed at room temperature (25 °C), and a full discharge was performed as a standard discharge before charging. First, in the case of the case without a rest period, for the test, 100%, 50%, and 20% were charged, and then 3% small discharge was performed immediately, and the final SOC was set based on the capacity. Then, after a 2-h rest period, the OCV was checked, and the

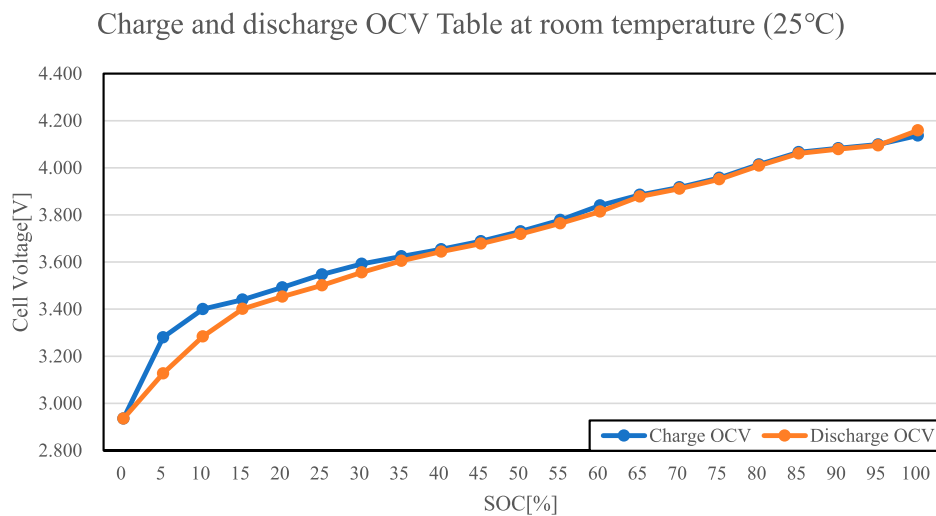


FIGURE 2
OCV Table for charge and discharge at 25 °C.

SOC was checked through the charge OCV Table and the discharge OCV Table, and compared with the final SOC.

Secondly, if there is a rest period, we charge to 100%, 50%, 20% destination for testing, and check the SOC with the charge OCV table after a rest period of 2 h, and perform a 3% discharge to set the final SOC. Then we check the rest period for 2 h, check the OCV, and check the SOC by looking at the charge OCV Table and the discharge OCV Table, and compare it with the final SOC.

Figure 3 shows the voltage change of a 3% small discharge after charging to 100% SOC, and Figure 4 is a graph showing the voltage change of a 3% small discharge after charging to 100% SOC and resting for 2 h. Table 1 summarizes the results shown in Figure 3. After charging to 100% SOC at 0.2C, a small 3% discharge is performed without a rest period. At this time, to confirm the effect of the C-rate of the small discharge, a 3% small discharge is performed at 0.2C, 0.5C, and 1C, and the Final SOC is calculated by capacity. The Final SOC is the result of subtracting the 3% small discharge. Then, the OCV, which is the stable cell voltage of the battery through a 2-h rest time, is measured, and the charge SOC and discharge SOC were confirmed using the charge OCV Table and the discharge OCV Table, respectively. The error was confirmed by comparing the charge SOC and discharge SOC values confirmed by the charge OCV Table and the discharge OCV Table with the Final SOC as the standard. Here, the error comparing the Final SOC and the charging SOC is denoted as Chg_SOC error, and the error comparing the Final SOC and the discharging SOC is denoted as Dhg_SOC error.

Table 2 summarizes the results shown in Figure 4. After charging to 100% SOC at 0.2C and resting for 2 h, the charge SOC is checked with the charge OCV Table. After that, in order to check the effect of the C-rate of the small discharge, a 3% small discharge is performed at 0.2C, 0.5C, and 1C, and the Final SOC is calculated. The Final SOC is the result of subtracting 3% from the previous charge SOC. Then, the OCV, which is the stable cell voltage of the battery through the 2-h rest period, is measured, and the charge SOC and discharge SOC are checked using the charge OCV Table and the discharge OCV

Table, respectively. The error is checked by comparing the charge SOC and discharge SOC values checked with the charge OCV Table and the discharge OCV Table based on the Final SOC.

As shown in Tables 1, 2, the error (Dhg_SOC error) of discharge SOC confirmed by the discharge OCV Table was small both in cases with and without a rest period between 100% charge and 3% small discharge. In addition, it was confirmed that there was no effect on the rest of the period. In addition, it can be confirmed that the effect of small discharge is large after 100% SOC charge. Conversely, the effect of 100% SOC charge is small. Therefore, if a small discharge occurs after 100% SOC charge, using the method of calculating SOC using the discharge OCV Table can reduce the SOC error.

Figure 5 shows the voltage change of a 3% small discharge after charging to 50% SOC, and Figure 6 is a graph showing the voltage change of a 3% small discharge after charging to 50% SOC and a 2-h rest period. Table 3 summarizes the results shown in Figure 5. After charging to 50% SOC at 0.2C, a 3% small discharge is performed without a rest period. At this time, to check the effect of the C-rate of the small discharge, a 3% small discharge is performed at 0.2C, 0.5C, and 1C, and the Final SOC is calculated with capacity. Then, the OCV, which is the stable cell voltage of the battery through a 2-h rest time, is measured, and the charge SOC and discharge SOC are checked using the charge OCV Table and the discharge OCV Table, respectively. The error was confirmed by comparing the charge SOC and discharge SOC values confirmed by the charge OCV Table and discharge OCV Table with the final SOC.

Table 4 summarizes the results shown in Figure 6. After charging to 50% SOC at 0.2C and having a 2-h rest period, the charge SOC is checked with the charge OCV Table. After that, in order to check the effect of the C-rate of the small discharge, 3% small discharges are performed at 0.2C, 0.5C, and 1C, and the Final SOC is calculated. Then, OCV, which is the stable cell voltage of the battery through a 2-h rest period, is measured, and the charge SOC and discharge SOC are checked using the charge OCV Table and the discharge OCV Table, respectively. The error was checked by comparing the charge

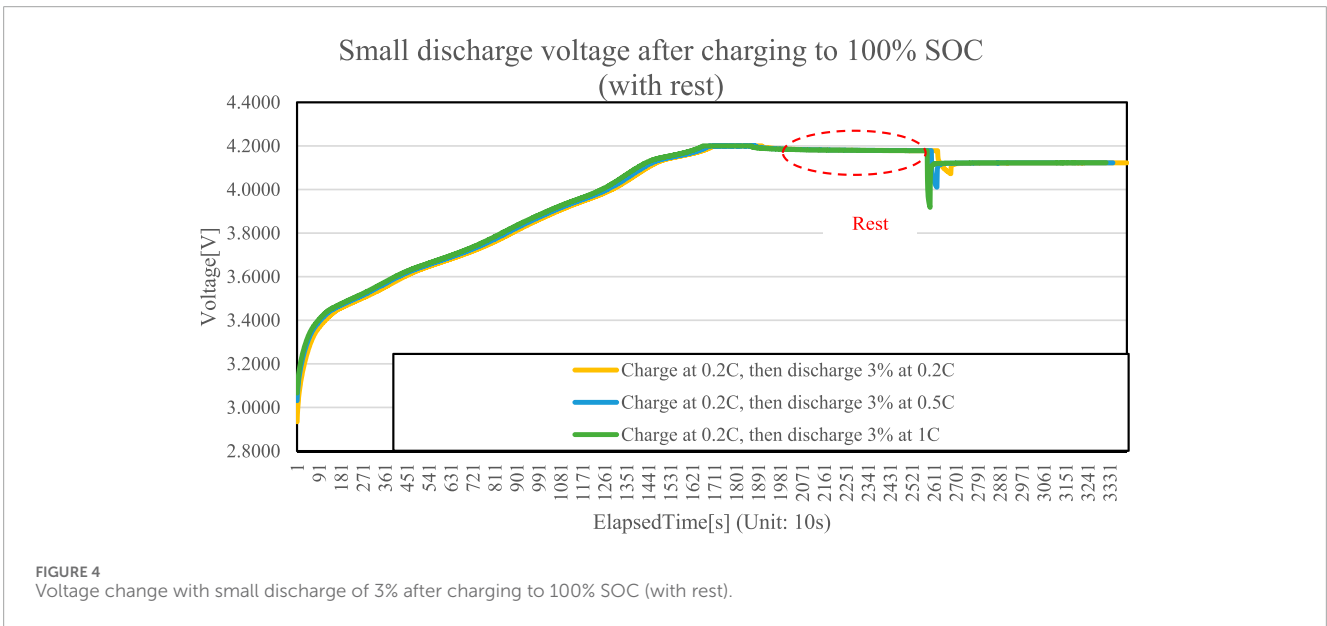
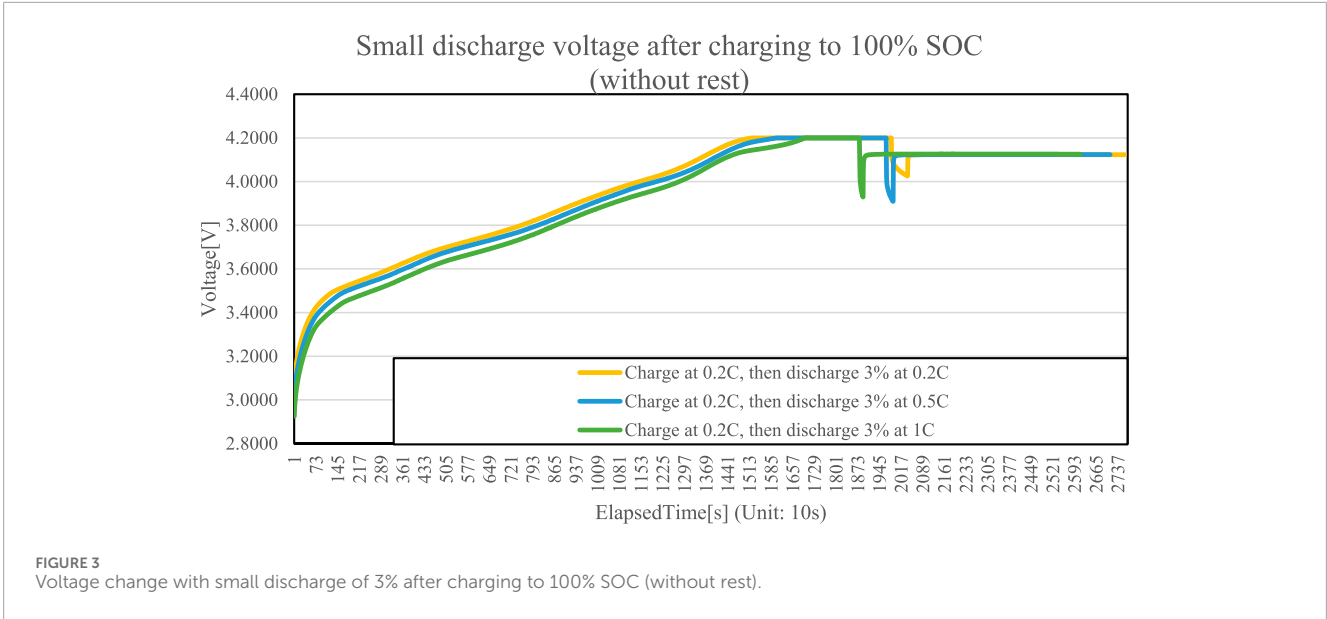


TABLE 1 SOC error according to voltage of small discharge of 3% after charging to 100% SOC (without rest).

| Charge | | | Small discharge | | | After 2 h of rest | | | SOC error | |
|--------|--------|-----------------------|-----------------|--------------------------|---------------|-------------------|------------------|---------------------|-------------------|-------------------|
| Mode | C-rate | Charging capacity [%] | C-rate | Discharging capacity [%] | Final SOC [%] | OCV [V] | Charging SOC [%] | Discharging SOC [%] | Chg_SOC error [%] | Dhg_SOC error [%] |
| CC-CV | 0.2C | 100% | 0.2C | 3% | 97.00% | 4.1228 | 98.13% | 97.17% | -1.13% | -0.17% |
| CC-CV | 0.2C | 100% | 0.5C | 3% | 97.00% | 4.1233 | 98.20% | 97.21% | -1.20% | -0.21% |
| CC-CV | 0.2C | 100% | 1C | 3% | 97.00% | 4.1256 | 98.50% | 97.39% | -1.50% | -0.39% |

TABLE 2 SOC error according to voltage of small discharge of 3% after charging to 100% SOC (with rest).

| Charge | | After 2 h of rest | | Small discharge | | | After 2 h of rest | | | SOC error | |
|--------|--------|-------------------|------------------|-----------------|--------------------------|---------------|-------------------|------------------|---------------------|-------------------|-------------------|
| Mode | C-rate | OCV [V] | Charging SOC [%] | C-rate | Discharging capacity [%] | Final SOC [%] | OCV [V] | Charging SOC [%] | Discharging SOC [%] | Chg_SOC error [%] | Dhg_SOC error [%] |
| CC-CV | 0.2C | 4.1779 | 100.00% | 0.2C | 3% | 97.00% | 4.1223 | 98.07% | 97.13% | -1.07% | -0.13% |
| CC-CV | 0.2C | 4.1783 | 100.00% | 0.5C | 3% | 97.00% | 4.1227 | 98.12% | 97.16% | -1.12% | -0.16% |
| CC-CV | 0.2C | 4.1781 | 100.00% | 1C | 3% | 97.00% | 4.1229 | 98.14% | 97.18% | -1.14% | -0.18% |

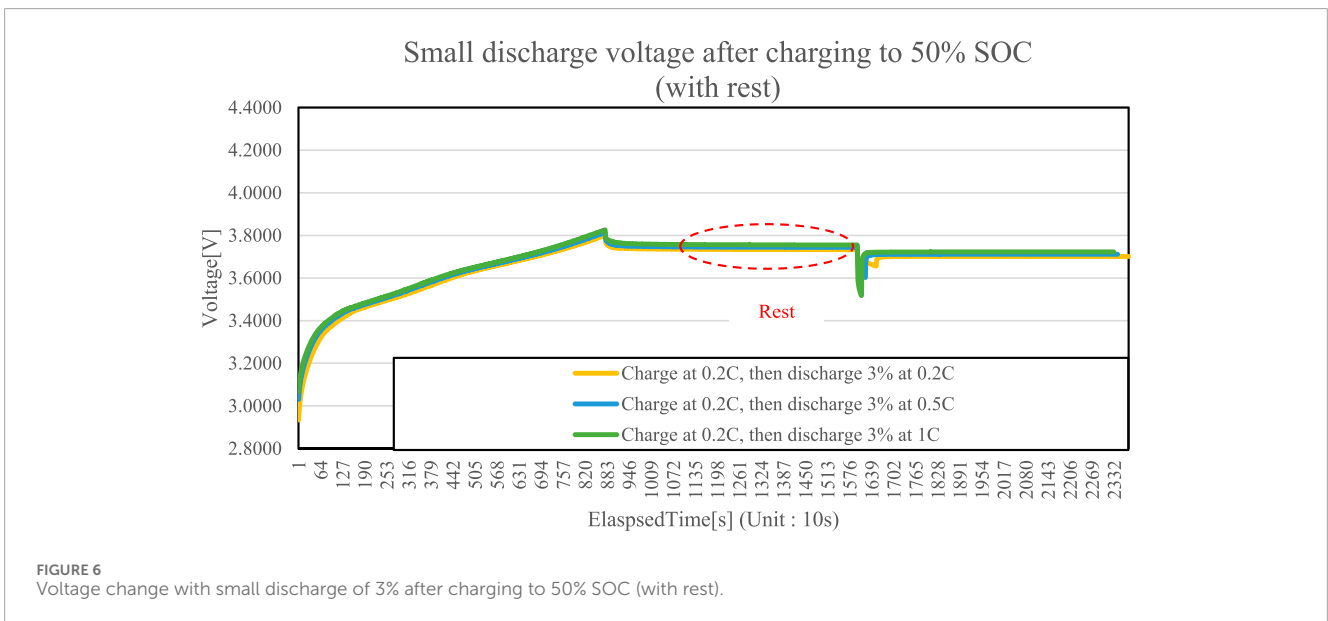
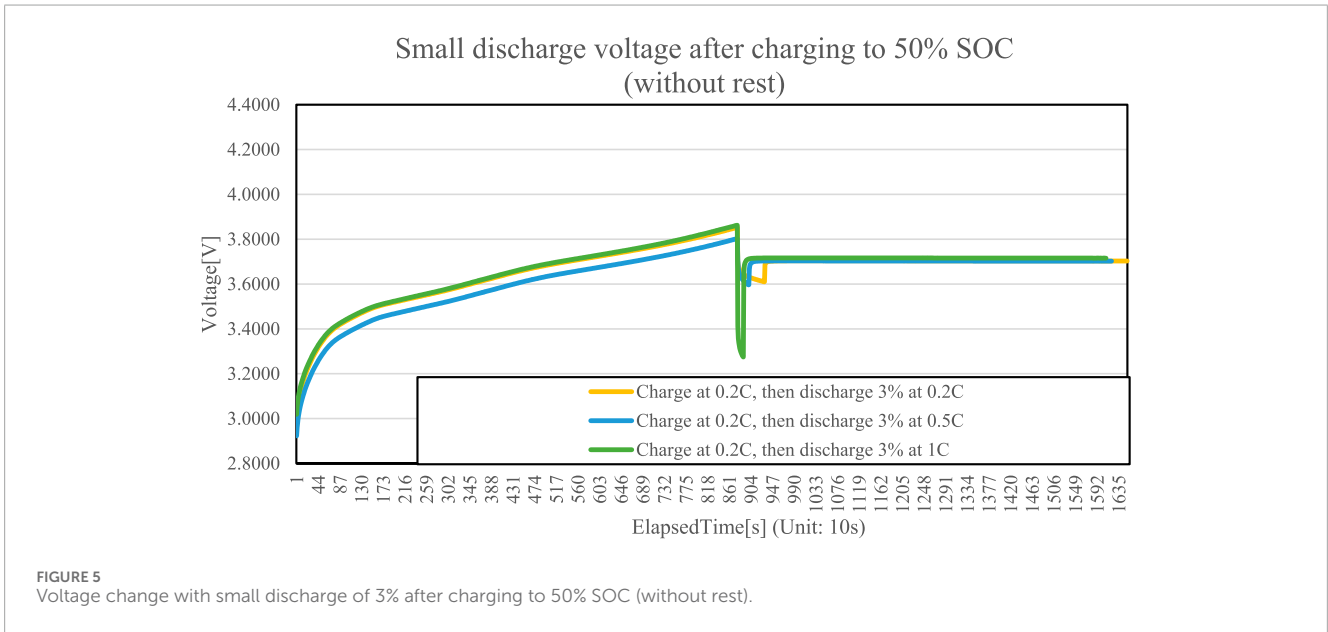
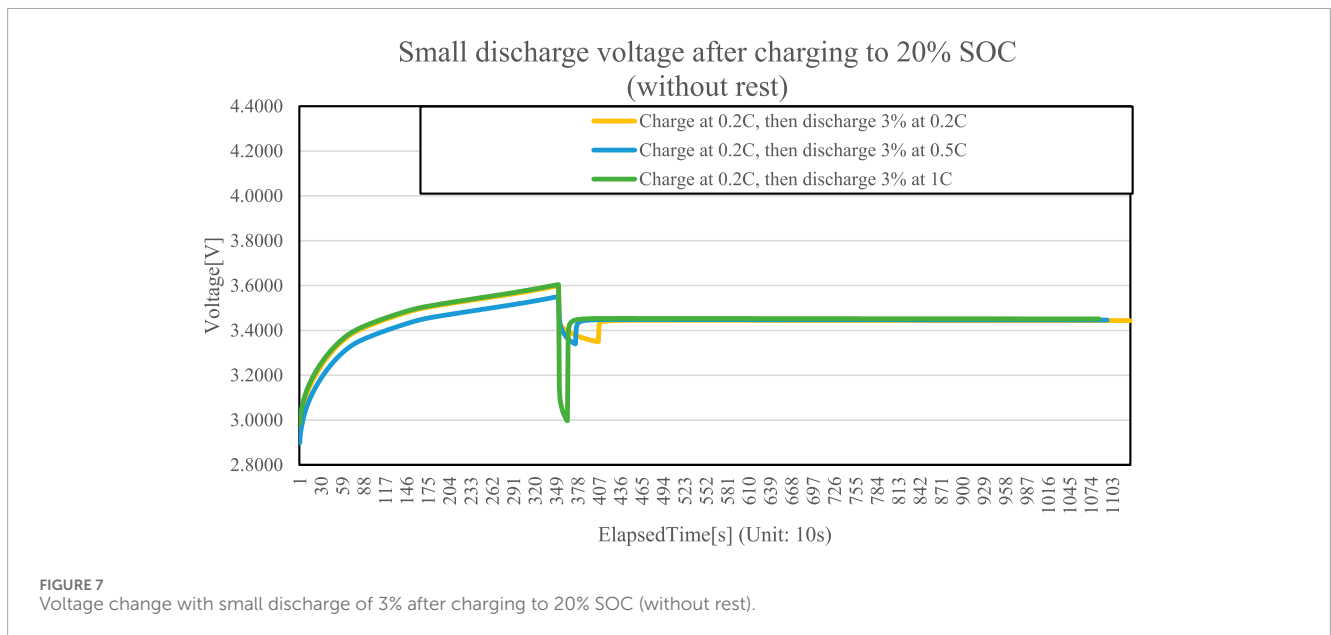


TABLE 3 SOC error according to voltage of small discharge of 3% after charging to 50% SOC (without rest).

| Charge | | | Small discharge | | | After 2 h of rest | | | SOC error | |
|--------|--------|-----------------------|-----------------|--------------------------|---------------|-------------------|------------------|---------------------|-------------------|-------------------|
| Mode | C-rate | Charging capacity [%] | C-rate | Discharging capacity [%] | Final SOC [%] | OCV [V] | Charging SOC [%] | Discharging SOC [%] | Chg_SOC error [%] | Dhg_SOC error [%] |
| CC | 0.2C | 50% | 0.2C | 3% | 47.00% | 3.7029 | 46.77% | 48.04% | 0.23% | -1.04% |
| CC | 0.2C | 50% | 0.5C | 3% | 47.00% | 3.7022 | 46.69% | 47.95% | 0.31% | -0.95% |
| CC | 0.2C | 50% | 1C | 3% | 47.00% | 3.7156 | 48.29% | 49.59% | -1.29% | -2.59% |

TABLE 4 SOC error according to voltage of small discharge of 3% after charging to 50% SOC (with rest).

| Charge | | After 2 h of rest | | Small discharge | | | After 2 h of rest | | | SOC error | |
|--------|--------|-------------------|------------------|-----------------|--------------------------|---------------|-------------------|------------------|---------------------|-------------------|-------------------|
| Mode | C-rate | OCV [V] | Charging SOC [%] | C-rate | Discharging capacity [%] | Final SOC [%] | OCV [V] | Charging SOC [%] | Discharging SOC [%] | Chg_SOC error [%] | Dhg_SOC error [%] |
| CC | 0.2C | 3.7331 | 50.32% | 0.2C | 3% | 47.32% | 3.7015 | 46.61% | 47.87% | 0.71% | -0.55% |
| CC | 0.2C | 3.7437 | 51.43% | 0.5C | 3% | 48.43% | 3.7116 | 47.81% | 49.10% | 0.62% | -0.67% |
| CC | 0.2C | 3.7548 | 52.58% | 1C | 3% | 49.58% | 3.7224 | 49.10% | 50.38% | 0.48% | -0.80% |



SOC and discharge SOC values checked with the charge OCV Table and the discharge OCV Table based on the Final SOC.

As a result of checking Table 3, 4, except for the results of charging at 0.2C, resting for 2 h, and discharging 3% at 0.2C, the remaining results show that the error in the charging SOC confirmed by the charging OCV Table is generally smaller, but the error in the SOC is not large, so it can be said to be similar. However, in order to reduce even a little error, it is necessary to check the SOC using the charging OCV Table.

Figure 7 is a graph showing the voltage change of a 3% small discharge after charging to 20% SOC, and Figure 8 is a graph showing the voltage change of a 3% small discharge after charging to 20% SOC and a 2-h rest period. Table 5 summarizes the results shown in Figure 7. After charging to 20% SOC at 0.2C, a 3% small discharge is performed without a rest period. At this time, in order to confirm the effect of the C-rate of the small discharge, a 3% small discharge is performed at 0.2C, 0.5C, and 1C, and the Final SOC is calculated with the capacity. Then, the OCV, which is the

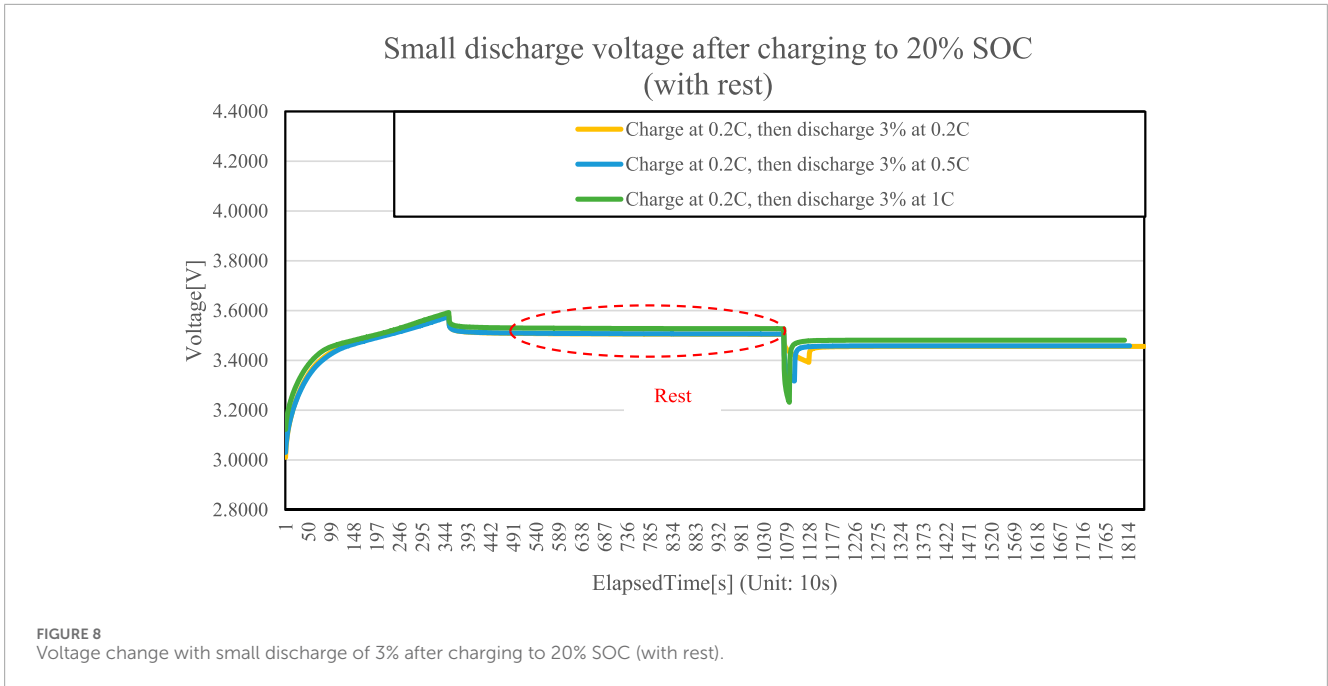


FIGURE 8 Voltage change with small discharge of 3% after charging to 20% SOC (with rest).

TABLE 5 SOC error according to voltage of small discharge of 3% after charging to 20% SOC (without rest).

| Charge | | | Small discharge | | | After 2 h of rest | | | SOC error | |
|--------|--------|-----------------------|-----------------|--------------------------|---------------|-------------------|------------------|---------------------|-------------------|-------------------|
| Mode | C-rate | Charging capacity [%] | C-rate | Discharging capacity [%] | Final SOC [%] | OCV [V] | Charging SOC [%] | Discharging SOC [%] | Chg_SOC error [%] | Dhg_SOC error [%] |
| CC | 0.2C | 20% | 0.2C | 3% | 17.00% | 3.4436 | 15.35% | 19.10% | 1.65% | -2.10% |
| CC | 0.2C | 20% | 0.5C | 3% | 17.00% | 3.4464 | 15.62% | 19.37% | 1.38% | -2.37% |
| CC | 0.2C | 20% | 1C | 3% | 17.00% | 3.4516 | 16.12% | 19.87% | 0.88% | -2.87% |

TABLE 6 SOC error according to voltage of small discharge of 3% after charging to 20% SOC (with rest).

| Charge | | After 2 h of rest | | Small discharge | | | After 2 h of rest | | | SOC error | |
|--------|--------|-------------------|------------------|-----------------|--------------------------|---------------|-------------------|------------------|---------------------|-------------------|-------------------|
| Mode | C-rate | OCV [V] | Charging SOC [%] | C-rate | Discharging capacity [%] | Final SOC [%] | OCV [V] | Charging SOC [%] | Discharging SOC [%] | Chg_SOC error [%] | Dhg_SOC error [%] |
| CC | 0.2C | 3.5045 | 21.14% | 0.2C | 3% | 18.14% | 3.4562 | 16.56% | 20.33% | 1.58% | -2.19% |
| CC | 0.2C | 3.5059 | 21.26% | 0.5C | 3% | 18.26% | 3.4583 | 16.76% | 20.55% | 1.50% | -2.29% |
| CC | 0.2C | 3.5272 | 23.20% | 1C | 3% | 20.20% | 3.4810 | 18.94% | 22.92% | 1.26% | -2.72% |

stable cell voltage of the battery through a 2-h rest time, is measured, and the charge SOC and discharge SOC are confirmed using the charge OCV Table and the discharge OCV Table, respectively. The error is confirmed by comparing the charge SOC and discharge SOC values confirmed by the charge OCV Table and the discharge OCV Table with the Final SOC as the standard.

Table 6 summarizes the results shown in Figure 8. After charging to 20% SOC at 0.2C and having a 2-h rest period, the charge

SOC is checked with the charge OCV Table. After that, in order to check the effect of the C-rate of the small discharge, 3% small discharges are performed at 0.2C, 0.5C, and 1C, and the Final SOC is calculated. Then, OCV, which is the stable cell voltage of the battery through a 2-h rest period, is measured, and the charge SOC and discharge SOC are checked using the charge OCV Table and the discharge OCV Table, respectively. The error was checked by comparing the charge SOC and discharge SOC values checked

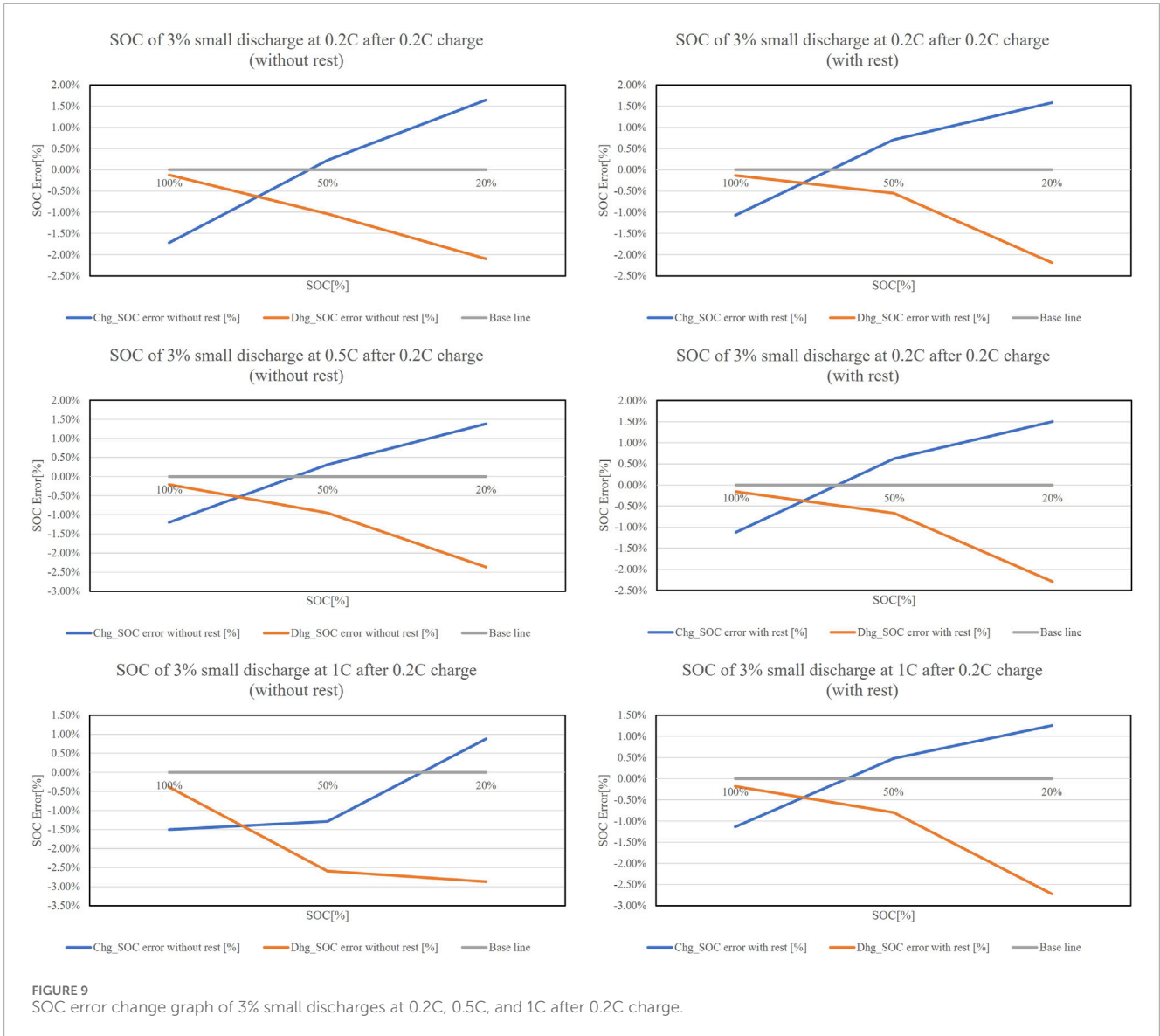


FIGURE 9 SOC error change graph of 3% small discharges at 0.2C, 0.5C, and 1C after 0.2C charge.

TABLE 7 Average SOC error results for 3% small discharges after charging.

| 0.2C charge SOC [%] | Small discharge | | Average SOC error | | | |
|------------------------|-----------------|----------|-----------------------------------|-----------------------------------|--------------------------------|--------------------------------|
| | C-rate | Capacity | Chg_SOC error without rest [%] | Dhg_SOC error without rest [%] | Chg_SOC error with rest [%] | Dhg_SOC error with rest [%] |
| 100% | 0.2C&0.5C&1C | 3% | -1.47% | -0.24% | -1.11% | -0.16% |
| 50% | 0.2C&0.5C&1C | 3% | -0.25% | -1.53% | 0.60% | -0.67% |
| 20% | 0.2C&0.5C&1C | 3% | 1.30% | -2.45% | 1.45% | -2.40% |

with the charge OCV Table and the discharge OCV Table based on the Final SOC.

As a result of checking Table 5, 6, it was confirmed that the error of the charge SOC confirmed by the charge OCV table

based on the Final SOC was small for both cases with and without a rest period between the 20% charge and the 3% small discharge. It can be confirmed that the 3% small discharge after the 20% SOC charge has no effect.

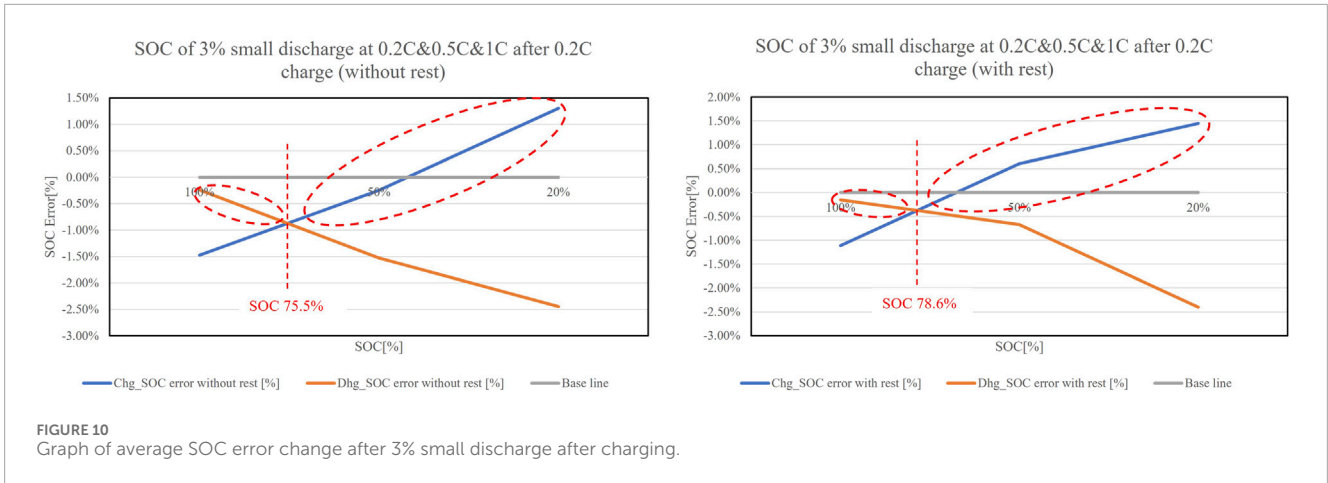


FIGURE 10 Graph of average SOC error change after 3% small discharge after charging.

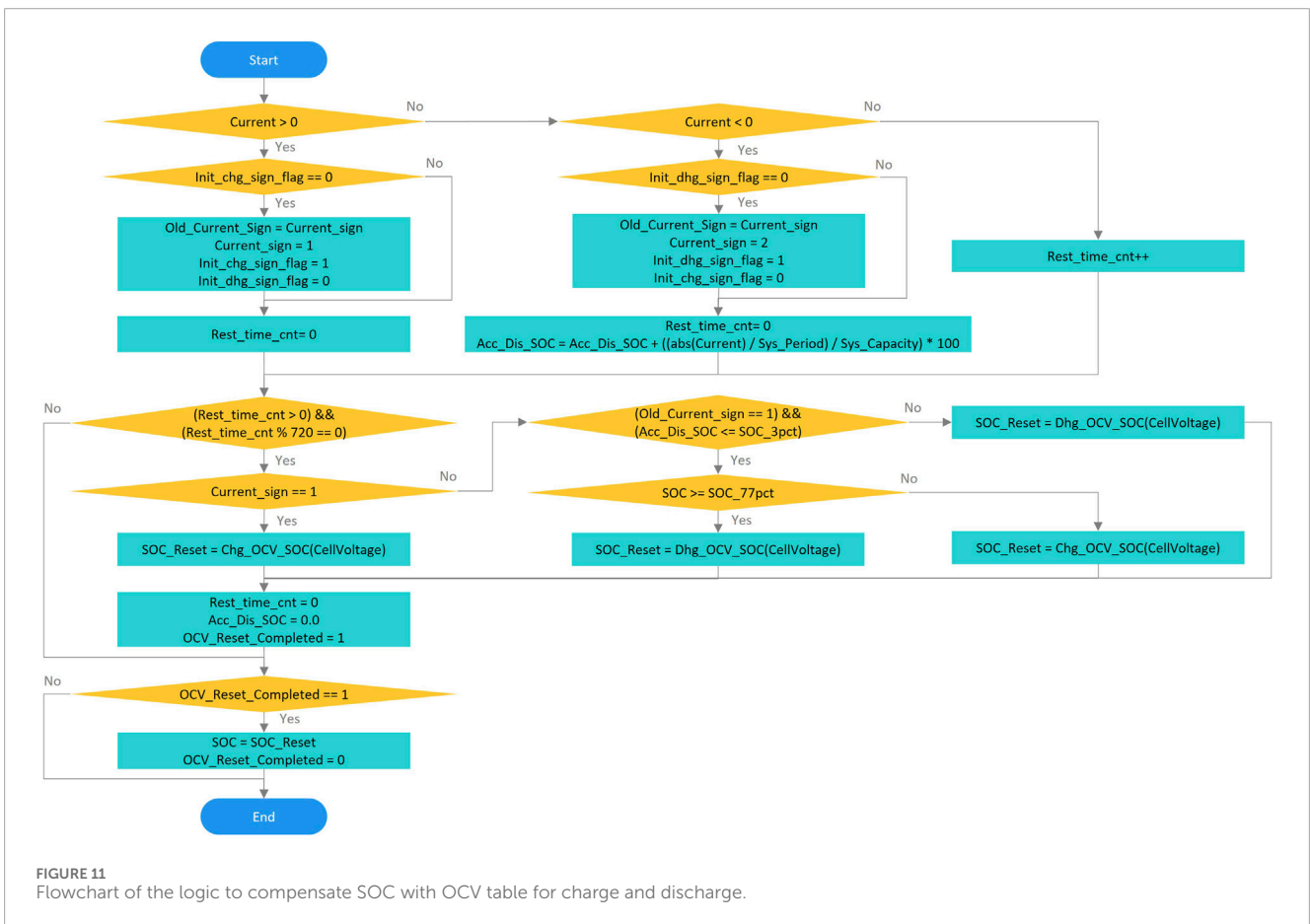


FIGURE 11 Flowchart of the logic to compensate SOC with OCV table for charge and discharge.

2.5 Application strategy based on results of small discharge after charging

Figure 9 is a graph connecting the SOC errors confirmed by the charge and discharge OCV Table for the cases of 3% small discharge with and without a 2-h pause at the 100%, 50%, and 20% points at 0.2C, 0.5C, and 1C, respectively. The left graph of Figure 9 is a SOC

error graph without a pause between charge and small discharge, and the right graph of Figure 9 is a SOC error graph with a 2-h pause between charge and small discharge. In the graphs, the charge SOC error (Chg_SOC error) is the SOC error confirmed by the charge OCV Table, and the discharge SOC error (Dhg_SOC error) is the SOC error confirmed by the discharge OCV Table. From the results of each graph, it can be confirmed that the SOC error

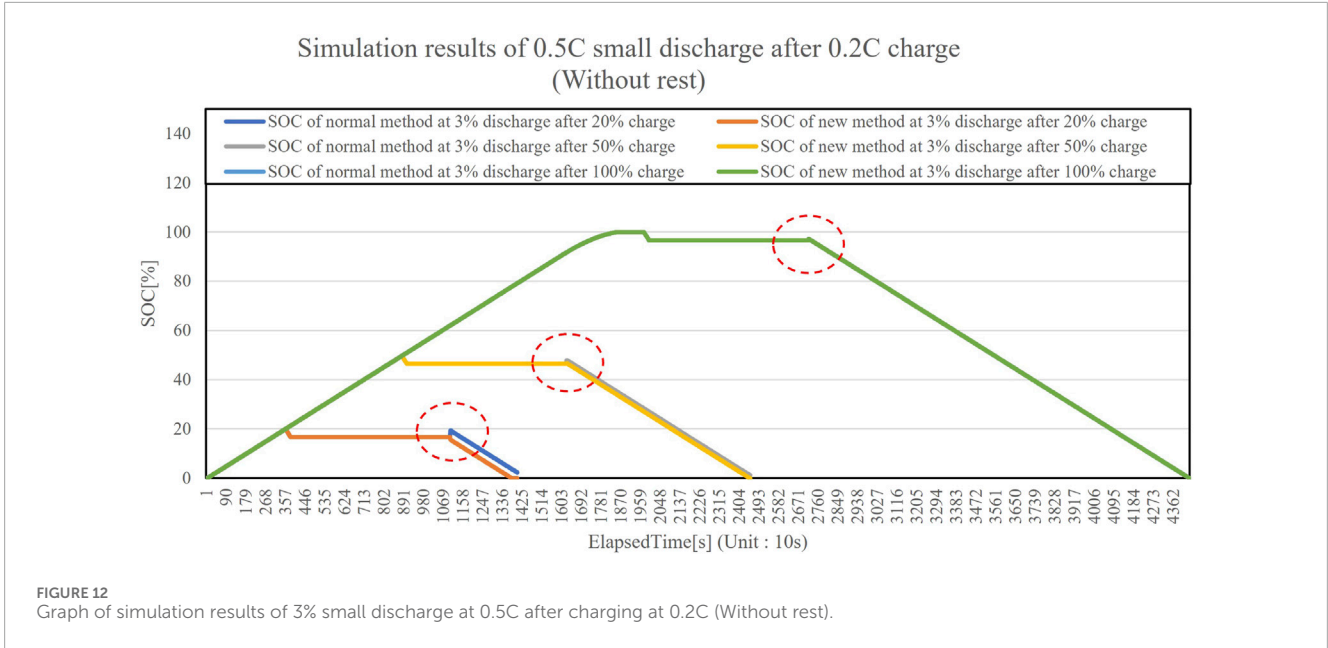


TABLE 8 Simulation results of 3% small discharge at 0.5C after charging at 0.2C (without rest).

| Charge | | After 2 h of rest | | Small discharge | | | After 2 h of rest | | | SOC error | |
|--------|--------|-----------------------|---------|-----------------|--------------------------|---------------|-------------------|-----------------------|--------------------|-----------------------------|--------------------------|
| Mode | C-rate | Charging capacity [%] | SOC [%] | C-rate | Discharging capacity [%] | Final SOC [%] | OCV [V] | Normal method SOC [%] | New method SOC [%] | Normal method SOC error [%] | New method SOC error [%] |
| CC | 0.2C | 20% | 20.00% | 0.5C | 3% | 17.00% | 3.4464 | 19.3% | 15.6% | -2.3% | 1.4% |
| CC | 0.2C | 50% | 50.00% | 0.5C | 3% | 47.00% | 3.7022 | 47.9% | 46.7% | -0.9% | 0.3% |
| CC-CV | 0.2C | 100% | 100.00% | 0.5C | 3% | 97.00% | 4.1233 | 97.2% | 97.2% | -0.2% | -0.2% |

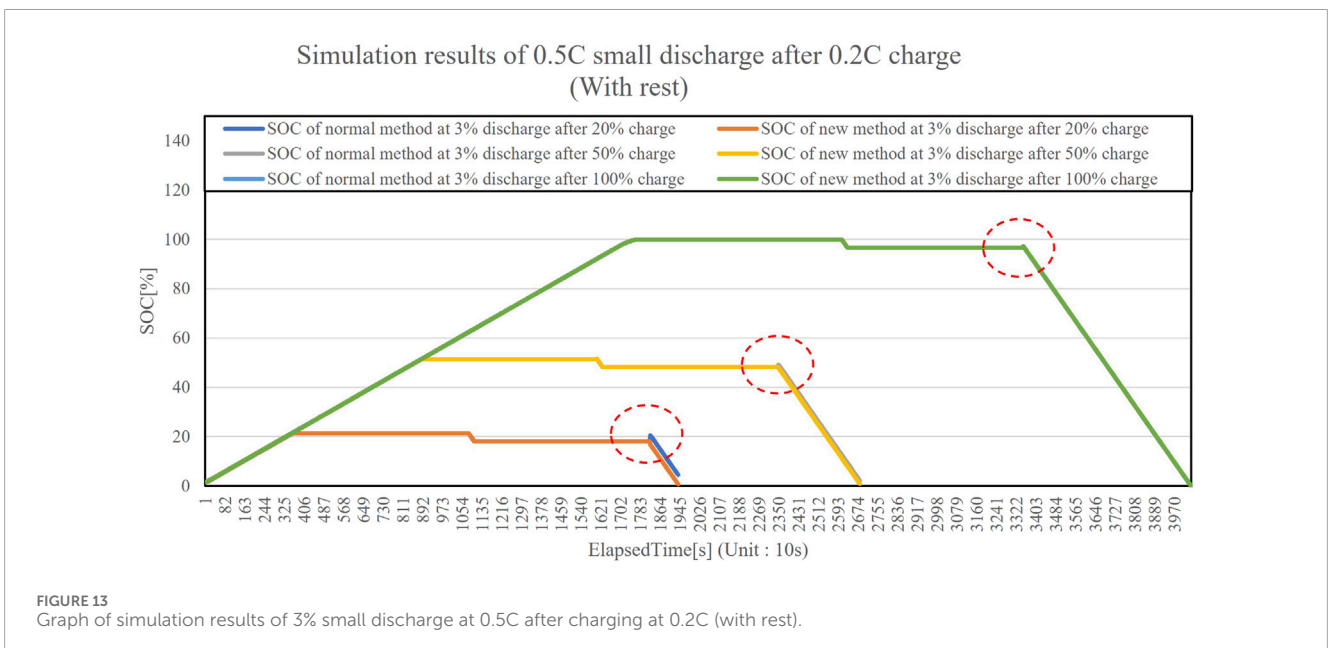


TABLE 9 Simulation results of 3% small discharge at 0.5C after charging at 0.2C (with rest).

| Charge | | After 2 h of rest | | Small discharge | | | After 2 h of rest | | | SOC error | |
|--------|--------|-------------------|------------------|-----------------|--------------------------|---------------|-------------------|-----------------------|--------------------|-----------------------------|--------------------------|
| Mode | C-rate | OCV [V] | Charging SOC [%] | C-rate | Discharging capacity [%] | Final SOC [%] | OCV [V] | Normal method SOC [%] | New method SOC [%] | Normal method SOC error [%] | New method SOC error [%] |
| CC | 0.2C | 3.5059 | 21.26% | 0.5C | 3% | 18.26% | 3.4583 | 20.5% | 16.7% | -2.2% | 1.6% |
| CC | 0.2C | 3.7437 | 51.43% | 0.5C | 3% | 48.43% | 3.7116 | 49.1% | 47.9% | -0.7% | 0.5% |
| CC-CV | 0.2C | 4.1783 | 100.00% | 0.5C | 3% | 97.00% | 4.1227 | 97.2% | 97.2% | -0.2% | -0.2% |

confirmed by the discharge OCV Table is smaller at high SOC and the SOC error confirmed by the charge OCV Table is smaller at low SOC, and it can be confirmed that generally all tests appear in a similar form.

Table 7 is a table expressing the test results without a rest time and with a 2-h rest time in Figure 9 as an average SOC error. The SOC error (Chg_SOC error) confirmed with the charge OCV Table in Table 7 changes from a positive error when the SOC is low to a negative error when the SOC is high both with no rest time and with a 2-h rest time. The SOC error (Dhg_SOC error) confirmed with the discharge OCV Table has a negative error both with no rest time and with a 2-h rest period, but the error decreases as the SOC increases. Based on these data, Figure 10 presents a graph. Looking at the change in the SOC error graph, it is distinguished based on SOC 75.5% when there is no rest time and based on SOC 78.5% when there is a 2-h rest time. As the SOC increases for each criterion, the SOC error (Dhg_SOC error) confirmed with the discharge OCV Table gets closer to the baseline (error 0%), and as the SOC decreases for each criterion SOC, the SOC error (Chg_SOC error) confirmed with the charge OCV Table gets closer to the baseline (error 0%).

Figure 11 is a flow chart of the logic for compensating the SOC with the charge and discharge OCV tables. The reason for checking whether the remainder of the rest time counter (Rest_time_cnt) variable divided by 720 is 0 is to perform the SOC compensation operation every 2 h since it operates in units of 10s. It can be changed depending on the operation time. In addition, if the discharge is less than 3% after charging and the current SOC is 77% or higher, the SOC is compensated with the discharge OCV Table, and if the current SOC is less than 77%, the SOC is compensated with the charge OCV Table. The reason for setting the SOC standard to 77% is that when there is no rest period, it is distinguished based on SOC 75.5%, and when there is a 2-h rest period, it is distinguished based on 78.5%, so the average value of 77% was applied. In addition, the logic was designed to compensate the SOC with the charge OCV Table if the previous state is charging, and to compensate the SOC with the discharge OCV Table if the previous state is discharging. The proposed flowchart was implemented and simulated in C code in a Visual Studio environment. The proposed logic was implemented in code to perform comparison with the general method, which simply compensates the SOC with the charge OCV Table if the previous state was a charge and compensates the SOC with the discharge OCV Table if the previous state was a discharge.

Figure 12 is a graph of the simulation results of 3% small discharge at 0.5C without rest time after charging at 0.2C, and Table 8 is a table summarizing the results. Figure 13 is a graph of the simulation results of 2% small discharge at 0.5C after charging at 0.2C and resting for 2 h, and Table 9 is a table summarizing the results. The simulation output results are designed to be rounded off from the second decimal place and expressed up to the first decimal place.

The simulation results without rest time in Table 8 show that near SOC 100%, the SOC error of both the conventional method and the proposed method was the same because they used the discharge OCV table. Near SOC 50%, the SOC error of the proposed method was 0.3% while the SOC error of the conventional method was -0.9%, which reduces the error of the proposed method. Near SOC 20%, the SOC error of the conventional method was -2.3% while the SOC error of the proposed method was 1.4%, which confirms that the accuracy of the proposed method was improved.

In the simulation results with the rest time in Table 9, the SOC error was the same for both the conventional method and the proposed method around 100% SOC because they both used the discharge OCV table. Around 50% SOC, the SOC error of the proposed method was 0.5% while that of the conventional method was -0.7%, which shows that the error of the proposed method was reduced. Around 20% SOC, the SOC error of the conventional method was -2.2% while that of the proposed method was 1.6%, which shows that the accuracy of the proposed method was improved.

3 Conclusion

In this study, a test was conducted to improve the accuracy of SOC correction using charge and discharge OCV tables when a small 3% discharge occurs after charging, as part of the OCV-based SOC correction function under battery stabilization conditions. This approach was compared with the conventional simple method. Since the timing of the rest period after charging can vary depending on the user, two test scenarios were considered: a 3% discharge performed immediately after charging, and a 3% discharge performed after a 2-h rest period. The test results showed similar patterns in both cases. Based on the average results of the two tests, it was found that in order to minimize SOC estimation error,

the discharge OCV table should be used when SOC is above 77%, while the charge OCV table is more appropriate when SOC is below 77%. A logic rule was developed based on these findings, and the corresponding code was implemented and validated through simulation.

Specifically, when charging to 100% SOC at 0.2C followed by an immediate 3% discharge, the proposed method reduced the SOC error to 1.4%, compared to -2.3% observed with the conventional method. Similarly, when the 3% discharge was performed after a 2-h rest, the SOC error was reduced to 1.6% with the proposed method, compared to -2.2% with the conventional method. The proposed approach can serve as a practical guideline for selecting the appropriate OCV table in both coulomb counting and Extended Kalman Filter (EKF)-based SOC estimation methods when a small discharge occurs after charging. By applying this logic, the accuracy and reliability of SOC estimation can be significantly enhanced.

This study has certain limitations that should be addressed in future research. The experiments were conducted at room temperature using fresh cells and thus did not consider potential variations in OCV–SOC behavior under extreme temperature conditions or with aged batteries. Additionally, although the proposed method estimates SOC on a per-cell basis and is robust to cell-to-cell variation, determining a representative SOC for the entire battery pack remains a separate challenge. Furthermore, the Thevenin equivalent model introduced for EKF-based SOC estimation was not supported by empirical parameter identification. Future work will include parameter extraction using the HPPC test protocol and sensitivity analysis under small current disturbances to enhance model accuracy and robustness. Future work will explore these aspects through extended testing under diverse conditions and pack-level SOC integration strategies.

Furthermore, while this study relies on OCV-based correction which typically requires a rest period, recent developments in advanced sensing technologies such as ultrasonic reflection waves offer promising potential for real-time SOC and temperature estimation without resting conditions. Future studies will consider integrating the proposed method with such sensor data fusion techniques to enhance the responsiveness and real-time applicability of battery management systems. In future work, the proposed correction logic will also be benchmarked against existing hybrid OCV strategies to evaluate its relative advantage. Additionally, we will investigate the practicality of segmented rest durations (e.g., intermittent idle periods during parking), which are more representative of real-world battery management system behavior in electric vehicles.

References

- Barai, A., Widanage, W. D., Marco, J., McGordon, A., and Jennings, P. (2015). A study of the open circuit voltage characterization technique and hysteresis assessment of lithium-ion cells. *J. Power Sources* 295, 99–107. doi:10.1016/j.jpowsour.2015.06.140
- Chatzigeorgiou, N. G., and Papadopoulos, A. I. (2024). A review on battery energy storage systems: applications, developments, and research trends. *Renew. Sustain. Energy Rev.* 155, 111–123.
- Cui, Z., Hu, W., Zhang, G., Zhang, Z., and Chen, Z. (2022). An extended kalman filter based SOC estimation method for Li-ion battery. *Energy Rep.* 8 (5), 81–87. doi:10.1016/j.egy.2022.02.116
- Dai, N., Zhang, Y., and Liu, Q. (2023). Research on fast-charging battery thermal management system based on refrigerant direct cooling. *Sci. Rep.* 13, 12456.
- Gabbar, H. A., Othman, A. M., and Abdussami, M. R. (2021). Review of battery management systems (BMS) development and industrial standards. *Technologies* 9 (2), 28. doi:10.3390/technologies9020028
- Jeong, Y.-M., Cho, Y.-K., Ahn, J.-H., Shin, S.-M., and Lee, B.-K. (2013). "SOC reset algorithm based enhanced OCV estimation for coulomb counting method," in *Power electronics conference*, 220–221.

Data availability statement

The original contributions presented in the study are included in the article/supplementary material, further inquiries can be directed to the corresponding author.

Author contributions

HS: Writing – original draft, Writing – review and editing. JK: Supervision, Writing – review and editing, Formal Analysis.

Funding

The author(s) declared that financial support was received for the research and/or publication of this article. This work was supported by a Korea University Grant.

Conflict of interest

The author(s) declared that this work was conducted in the absence of any commercial or financial relationships that could be construed as a potential conflict of interest.

Generative AI statement

The author(s) declared that generative AI was not used in the creation of this manuscript.

Any alternative text (alt text) provided alongside figures in this article has been generated by Frontiers with the support of artificial intelligence and reasonable efforts have been made to ensure accuracy, including review by the authors wherever possible. If you identify any issues, please contact us.

Publisher's note

All claims expressed in this article are solely those of the authors and do not necessarily represent those of their affiliated organizations, or those of the publisher, the editors and the reviewers. Any product that may be evaluated in this article, or claim that may be made by its manufacturer, is not guaranteed or endorsed by the publisher.

- Jeong, Y. M., Cho, Y. K., Ahn, J. H., Ryu, S. H., and Lee, B. K. (2014). "Enhanced coulomb counting method with adaptive SOC reset time for estimating OCV" in 2014 IEEE energy conversion congress and exposition (ECCE), Pittsburgh, PA, USA, 14-18 September 2014 (IEEE), 1313-1318.
- Ku, H. K., Seo, H. R., and Kim, J. M. (2015). Lithium-ion battery energy storage system for power quality improvement in electrical propulsion ships. *Trans. Korean Inst. Power Electron.* 20 (4), 351-355. doi:10.6113/tkpe.2015.20.4.351
- Lee, S., Kim, J., and Cho, B. H. (2005). Maximum pulse current estimation for high accuracy power capability prediction of a Li-Ion battery. *Microelectron. Reliab.* 55 (3-4), 572-581. doi:10.1016/j.microrel.2014.12.016
- Lee, S. J., Kim, J. H., Lee, J. M., and Cho, B. H. (2007). "The state and parameter estimation of an Li-ion battery using a new OCV-SOC concept," in IEEE power electronics specialists conference, Orlando, FL, United States, 17-21 June 2007 (IEEE), 2799-2803.
- Lu, L., Han, X., Li, J., Hua, J., and Ouyang, M. (2013). A review on the key issues for lithium-ion battery management in electric vehicles. *J. Power Sources* 226, 272-288. doi:10.1016/j.jpowsour.2012.10.060
- Misyris, G. S., Marinopoulos, A., Doukas, D. I., Tegnér, T., and Labridis, D. P. (2017). On battery state estimation algorithms for electric ship applications. *Electr. Pow. Syst. Res.* 151, 115-124. doi:10.1016/j.epsr.2017.05.009
- Ng, K. S., Moo, C.-S., Chen, Y.-P., and Hsieh, Y. C. (2009). Enhanced coulomb counting method for estimating state-of-charge and state-of-health of lithium-ion batteries. *Appl. Energy* 86, 1506-1511. doi:10.1016/j.apenergy.2008.11.021
- Omariba, Z. B., Zhang, L., and Sun, D. (2019). Review of battery cell balancing methodologies for optimizing battery pack performance in electric vehicles. *IEEE Access* 7, 129335-129352. doi:10.1109/access.2019.2940090
- Ovejas, V. J., Garcés, L. J., del Real, A. J., and Bordons, C. (2019). Effects of cycling on lithium-ion battery hysteresis and overvoltage. *Sci. Rep.* 9, 14875. doi:10.1038/s41598-019-51474-5
- Sato, S., and Kawamura, A. (2002). A new estimation method of state of charge using terminal voltage and internal resistance for lead acid battery. *Proc. IEEE PCC 2*, 565-570. doi:10.1109/pcc.2002.997578
- Shrivastava, P., Soon, T. K., Idris, M. Y. I. B., and Mekhilef, S. (2019). Overview of model-based online state-of-charge estimation using kalman filter family for lithium-ion batteries. *Renew. Sustain. Energy Rev.* 113, 109233. doi:10.1016/j.rser.2019.06.040
- Song, H. (2025). Research on the application of charge and discharge OCV to improve SOC accuracy of lithium-ion battery systems. *J. Energy Eng.* 34 (1), 42-53. doi:10.5855/energy.2024.34.1.042
- Song, H., Kahng, H.-K., and Kim, J. (2025). State of health estimation and error reduction method for embedded lithium battery system. *J. Energy Storage* 109, 115243. doi:10.1016/j.est.2024.115243
- Xiong, R., He, H., Guo, H., and Ding, Y. (2011). Modeling for lithium-ion battery used in electric vehicles. *Procedia Eng.* 15, 2869-2874. doi:10.1016/j.proeng.2011.08.540
- Yang, J., Xia, B., Huang, W., and Mi, C. (2017). "Improved OCV measurement method with reduced relaxation time," in 2017 IEEE Transportation Electrification Conference and Expo, Asia-Pacific (ITEC Asia-Pacific), Harbin, China, 07-10 August 2017 (IEEE).
- Zhang, C., Jiang, J., Zhang, L., Liu, S., Wang, L., and Loh, P. (2016). A generalized SOC-OCV model for lithium-ion batteries and the SOC estimation for LNMCO battery. *Energies* 9 (11), 900. doi:10.3390/en9110900
- Zhang, S., Xie, C., Zeng, C., and Quan, S. (2019). SOC estimation optimization method based on parameter modified particle kalman filter algorithm. *Clust. Comput.* 22, 6009-6018. doi:10.1007/s10586-018-1784-0
- Zhou, Z., Cui, Y., Kong, X., Li, J., and Zheng, Y. (2020). A fast capacity estimation method based on open circuit voltage estimation for LiNixCoyMn1-xy battery assessing in electric vehicles. *J. Energy Storage* 32, 101830. doi:10.1016/j.est.2020.101830
- Zhou, M.-Y., Zhang, J. B., Ko, C. J., and Chen, K. C. (2023). Precise prediction of open circuit voltage of lithium ion batteries in a short time period. *J. Power Sources* 553, 232295. doi:10.1016/j.jpowsour.2022.232295